SEISMIC NOISE ATTENUATION USING AN IMPROVED VARIATIONAL MODE DECOMPOSITION METHOD

YATONG ZHOU and YUE CHI

School of Electronic and Information Engineering, Hebei University of Technology, Xiping Road No. 5340, Beichen District, Tianjin 300401, P.R. China. zyt_htu@126.com

(Received September 5, 2018; revised version accepted October 31, 2019)

ABSTRACT

Zhou, Y.T. and Chi, Y., 2020. Seismic noise attenuation using an improved variational mode decomposition method. *Journal of Seismic Exploration*, 29: 29-47.

Seismic noise suppression is an important step in the seismic imaging community. We propose a dip-separated denoising method to attenuate spatially incoherent random noise. The variational mode decomposition (VMD) method is used to decompose the seismic data into different dip bands. It has a solid theoretical foundation of mathematics and high calculation efficiency. Besides, compared with the recursive mode decomposition algorithms, e.g., the EMD and EEMD methods, it has advantages in solving the mode mixing problem and more powerful anti-noise performance. The VMD method can adaptively decompose a seismic signal into several intrinsic mode functions (IMF). Decomposing the seismic data into oscillating IMF components is equivalent of decomposing the seismic data into different dipping components. To automatically define the optimal number of most oscillating components, we design the Kurtosis method. To eliminate the errors caused by end effect, we use a waveform matching extension algorithm to improve the VMD. The singular spectrum analysis (SSA) method is used to approximate the low-rank components in each separated dip band. In this paper, a simulated seismic dataset and a real seismic dataset are analyzed by the proposed algorithm. The results indicate that the proposed algorithm is robust to noise and has high de-noising precision.

KEY WORDS: random noise suppression, variational mode decomposition, singular spectrum analysis, intrinsic mode functions.

0963-0651/20/$5,00 © 2020 Geophysical Press Ltd.

INTRODUCTION

Random noise attenuation plays an indispensable role in seismic data processing. The useful signal that is mixed with the ambient random noise is often neglected and thus may cause confusion between seismic events and artifacts in the final migrated image (Canales, 1984; Gan et al., 2016d; Wu and Bai, 2018c). Enhancing the useful signal while attenuating random noise can help reduce interpretation difficulties and risks for oil & gas detection (Liu et al., 2012; Chen and Fomel, 2015; Chen et al., 2016b; Chen, 2018a,b; Wu and Bai, 2018a,b,d; Wang et al., 2018; Bai et al., 2019).

The widely used frequency-space prediction filtering (Canales, 1984) can achieve good results for linear events but may fail in handling complex or hyperbolic events (Liu et al., 2012). A mean or median filter (Gan et al., 2016c; Bai and Wu, 2017; Chen et al., 2019) is often used to attenuate specific types of random noise, e.g., a mean filter is effective in attenuating Gaussian white noise, and a median filter can remove random spikes with excellent performance (Chen et al., 2017c). An eigen-image based approach (Bekara and van der Baan, 2007), sometimes referred to as global singular value decomposition (SVD), is effective for horizontal-events in seismic profiles, but cannot be adapted to geologically complicated structures. An enhanced version of this method turns global SVD to local SVD (Bekara and van der Baan, 2007), where a dip steering process is performed in each local processing window to enhance the locally coherent events. The problem with local SVD is that only one slope component for each processing window is allowed, and also the optimal size of each processing window is often difficult to select. Structure-oriented SVD is designed specifically for seismic data by applying the SVD filtering along the morphological structure direction of seismic data (Bai et al., 2018b). Matrix completion via f-x domain singular spectrum analysis (SSA) can handle complex dipping events well by extracting the first several eigen-components after SVD for each frequency slice (Chen et al., 2016c; Xue et al., 2016; Zhang et al., 2016; Bai et al., 2018b,a; Huang et al., 2017b). The f-x SSA approach is based on a pre-defined rank of the seismic data. The rank here denotes the number of linear components in the seismic data. However, for complex seismic data, the rank is hard to select, and for curved events, the rank tends to be high and thus will involve a serious rank-mixing problem. Chen and Fomel (2015) proposed a two-step processing strategy to guarantee no coherent signal is lost in the removed noise. More advanced and recent denosing methods from various fields in seismics and micro-seismics include new sparse domain shrinking (Zhang et al., 2017; Wang et al., 2017; Zu et al., 2017b,c; Bai and Wu, 2018), e.g., seislet (Fomel and Liu, 2010; Chen et al., 2014; Gan et al., 2015; Liu et al., 2016c; Gan et al., 2016a,b), EMD-seislet (Chen and Fomel, 2018), curvelet transform (Cand`es et al., 2006; Zu et al., 2016, 2017a), sparse dictionaries (Siahsar et al., 2017a,b; Chen, 2017; Lv and Bai, 2018), mathematical morphology (Li et al., 2016a,b; Huang et al., 2017c, 2018), plane-wave orthogonal polynomial transform (Chen et al., 2018), clustering-

based method (Chen and Song, 2018), and double least-squares projections method (Huang et al., 2017a).

With empirical mode decomposition (EMD) algorithm, a signal can be decomposed into series of intrinsic mode functions (IMFs) according to time domain characteristics of the signal (Huang et al., 1998; Chen et al., 2017b). It does not need to set any basis functions a priori, and it also has advantages in dealing with non-stationary and non-linear signals. However, this algorithm has the mode mixing problem, and it cannot completely extract the subsurface reflection response from the low SNR and complex seismic signals (Chen and Ma, 2014; Huang et al., 2017d). For ensemble empirical mode decomposition (EEMD) algorithm (Chen et al., 2017d), the white Gaussian noise with uniform distribution is added to original signals, which makes the original signals have a uniformly distributed decomposition scale. It can smooth abnormal signals such as pulse and discontinuous signals and avoid mode mixing effectively. Nevertheless, the introduction of white Gaussian noise destroys the purity of the original signals (Chen et al., 2016a, 2017a). The basic idea of variational mode decomposition (VMD) is to solve the L2 norm squared of the gradient of demodulation signal variational problems. An iterative method is employed to search the optimal solution of the variational problem to realize signal decomposition. The VMD has a solid foundation of mathematical and can solve the problem of mode mixing (Dragomiretskiy and Zosso, 2014; Liu et al., 2016a, 2017, 2016b, 2018). In comparison with the above methods, the VMD algorithm exhibits two advantages. Firstly, it has a solid theoretical foundation of mathematics and high calculation efficiency. Secondly, compared with the recursive mode decomposition algorithms, e.g., the EMD and EEMD methods, it has advantages in solving the mode mixing problem and more powerful anti-noise performance. Whereas, the VMD algorithm still has a drawback that the mode number needs to be set artificially before decomposition. The mode number is difficult to estimate when a signal is a complex nonlinear and non-stationary one. If the mode number is small, multiple components of the signal may exist in one mode simultaneously. Otherwise, one component of the signal will exist in multiple modes. Therefore, in compensating the drawbacks of the VMD method, some subsequent filtering methods need to be combined with the VMD decomposition in order to effectively suppress random noise.

Usually, the low-frequency IMFs are complex. The seismic signal is coupled with random noise in the seismic frequency band. The coupling relationships between the seismic signal and random noise are complex, which the low-frequency IMFs have a dense frequency feature. However, the VMD method can only be used to decompose the signal in a complete space and it cannot separate the weak seismic signal from such a complex signal with dense frequency noise. Therefore, the low-frequency random noise cannot be effectively separated by the VMD algorithm. To overcome the aforementioned shortcomings, the SSA) algorithm (Vautard et al., 1992;

Dragomiretskiy and Zosso, 2014; Siahsar et al., 2017c) is applied to further filter the low-frequency noise from the de-noised signal by the VMD algorithm. SSA method can describe the essential difference of the singular values between useful components and noise components, and a signal can be decomposed into an uncorrelated useful signal subspace and a noise subspace in time domain. Therefore, the low-frequency noise can be filtered by the SSA algorithm.

The rest of the paper is organized as follows: in the first section, we introduce the improved VMD algorithm and the SSA algorithm; in the next section, we use both synthetic and real seismic data examples to demonstrate the performance of the proposed combined method, finally, we draw some key conclusions.

THEORY

The variational mode decomposition method

VMD assumes that f is composed of a given number of modes $u_k(t)$. These modes are called intrinsic mode functions (IMFs). The bandwidth of each IMF is estimated and the constrained variational problem is given by Dragomiretskiy and Zosso (2014):

$$\min_{\{u_k\},\{w_k\}} \left\{ \sum_k \left\| \partial_t \left[\delta(t) + \frac{j}{\pi t} \right] * u_k(t) \right] e^{-jw_k t} \right\|_2^2 \right\}$$
$$s.t. \quad \sum_k u_k(t) = f. \qquad (1)$$

where $\| \cdot \|_2$ is the L2 norm. $\delta(t)$ is the unit pulse function. j is the imaginary unit. $*$ is convolution. ∂_t is partial derivative of time t. $\{u_k(t)\} = \{u_1(t), \cdots, u_k(t)\}$ and $\{w_k\} = \{w_1, \cdots, w_k\}$ are shorthand notions for the set of all modes and their center frequencies, respectively. f is the extended signal.

To solve the constrained variational problem, the augmented Lagrange is introduced and the non-constrained variational problem is obtained

$$L(\{u_k\},\{w_k\},\lambda) = \alpha \sum_k \left\| \partial_t \left[\left(\delta(t) + \frac{j}{\pi t} \right) * u_k(t) \right] e^{-jw_k t} \right\|_2^2 + \left\| f(t) - \sum_k u_k(t) \right\|_2^2 + \langle \lambda(t), f(t) - \sum_k u_k(t) \rangle, \quad (2)$$

where α denotes quadratic penalty factor. λ is Lagrange multipliers. ⟨, ⟩ is the inner product. The saddle point of eq. (2) is the optimal solution of the original problem, which can be obtained using the alternating direction method of multipliers (ADMM). All the modes can be obtained from eq. (3) in the frequency domain through updating each mode u_k and its center frequency w_k constantly:

$$\hat{u}_k^{n+1}(w) = \frac{\hat{f}(w) - \sum_{i=1}^{k-1} \hat{u}_i^{n+1}(w) - \sum_{i=k+1}^{K} \hat{u}_i^n(w) + \frac{\hat{\lambda}^n(w)}{2}}{1 + 2\alpha(w - w_k^n)^2}. \quad (3)$$

The new center frequency w^{n+1} is placed at the center of gravity of the corresponding power spectrum of mode, which can be updated by:

$$w_k^{n+1} = \frac{\int_0^\infty w \left| \hat{u}_k^{n+1}(w) \right|^2 dw}{\int_0^\infty \left| \hat{u}_k^{n+1}(w) \right|^2 dw}. \quad (4)$$

From the above decomposition process, the *K* must be determined a priori. However, various algorithms of selecting *K* are proposed in the literatures. They suffer from different drawbacks. Because of the difficulty in selecting *K*, the performance after VMD is almost always far from being perfect. In this paper, we use a different way to solve this problem. We can use a relatively large number of *K* and removes the most oscillating components, and leaves less oscillating components dealt with by a secondary processing step.

However, the number of most oscillating components that are used for reconstruction still need to be defined in advance. In this paper, we propose a new strategy to pick the most significant IMFs that can be used for reconstructing the signals. The new strategy is based on the Kurtosis calculation. Kurtosis is a way to measure the ”tailedness” of the decomposed component, which is defined as:

$$K(\mathbf{x}) = \frac{\mathrm{E}[(\mathbf{x}-\mu)^4]}{(\mathrm{E}[(\mathbf{x}-\mu)^2])^2} \quad , \tag{5}$$

where E denotes the expectation, μ denotes the mean of the series x. In the proposed method, we assume that the decomposed component (IMF) using the VMD algorithm has different Kurtosis value. The high kurtosis value corresponds to more dominant signal component while the low kurtosis value corresponds to more oscillating noise component. We can define a kurtosis threshold to select the most significant components for signal reconstruction. In this paper, we define the Kurtosis value as half of the maximal kurtosis value.

In this paper, we use the SSA method to further remove the residual noise in the low-frequency components after VMD decomposition. To eliminate the errors caused by end effect, we use a waveform matching extension algorithm to improve the VMD, i.e., to extend to the original time series around the boundaries so that the extended waveforms best match the boundary waveforms.

The singular spectrum analysis method

Let the time series of a signal de-noised by the VMD be $\{h_i,\ i = 1,2,\cdots,N\}$, and then it is used to calculate a Hankel matrix with the expression:

$$\mathbf{H} = \begin{pmatrix} h_1 & h_2 & \cdots & h_K \\ h_2 & h_3 & \cdots & h_{K+1} \\ \vdots & \vdots & \ddots & \vdots \\ h_L & h_{L+1} & \cdots & h_N \end{pmatrix} \quad , \tag{6}$$

where L represents window length parameter and $1 < L < N$. K is defined a $N - L + 1$. The delay value is 1. The matrix $\mathbf{H}$ is referred to the trajectory matrix. The resulting trajectory matrix is then decomposed by means of singular value decomposition (SVD) and $\mathbf{H}$ can be rewritten as:

$$\mathbf{H} = \sum_{i=1}^{d} \mathbf{H}_i, \text{with}, \mathbf{H}_i = \sqrt{\lambda_i}\mathbf{U}_i\mathbf{V}_i^T \quad , \tag{7}$$

where d = rank($\mathbf{H}$) and it is the number of eigen-components or modes with non-zero eigenvalue. λ_i are the singular values sorted in the descending

order. $\mathbf{U_i}$ and $\mathbf{V_i}$ are respectively the associated left and right singular vectors. The group denoted by $\{\sqrt{\lambda_i}\mathbf{U_i}\mathbf{V}_i^T\}$ is called the ith eigentriple. Then the elementary matrices $\mathrm{H_i}$ (i = 1, 2, 3, $\cdots$, d) are split into signal and noise groups. However, the important step is to determine a subset of eigentriple that encompass the dominant variation in H. This amounts to approximating matrix $\widetilde{\mathbf{H}}$ by the summation of the first r elementary matrices, using the following equation: $\widetilde{\mathbf{H}} = \sum_{i=1}^{r}\sqrt{\lambda_i}\mathbf{U_i}\mathbf{V}_i^T$, where $\widetilde{\mathbf{H}}$ is attributed to signal, and r denotes the number of eigentriples selected for signal reconstruction, and the residual $\mathbf{R} = \sum_{i=r+1}^{d}\sqrt{\lambda_i}\mathbf{U_i}\mathbf{V}_i^T$ is taken as noise.

Selection of eigentriples r is the kernel of signal extraction. If r is small, part of the useful signal will be lost, and if r is large, noise will be introduced. In this paper, the singular value difference spectrum is introduced to select r. When the signal is decomposed, singular values are arranged in a descending order and a matrix $\mathbf{S} = \{\sqrt{\lambda_1}, \sqrt{\lambda_2}, \cdots \sqrt{\lambda_d}\}$ is formed.

Let $b_i = \sqrt{\lambda_i} - \sqrt{\lambda_{i+1}}\ (i = 1,2,\cdots, d-1)$, and vector $\mathbf{B} = \{b_1, !_2, \cdots ! b_{d-1}\}$, called the singular value difference spectrum, is formed to describe the variation of every adjacent singular values. We propose to use the sharp peak $\max(\mathrm{b_i}) = \mathrm{b_r}$, i = 1,2,$\cdots$,d – 1, to represent the boundary between signal and noise. That is to say, we use the first r components to reconstruct the signal.

Hybrid improved VMD and SSA method

The hybrid method is detailed as follows:

1. Transform seismic data from t – x domain to f – x domain.
2. For each frequency slice in the f – x domain, use VMD to decompose the seismic data into different IMFs.

(a) Calculate the kurtosis metrics for each VMD components and define the number of most oscillating components.
(b) Treat the most oscillating components (that corresponds to the highest frequency/wavenumber) as noise and reject it.
(c) For the rest components, construct Hankel matrices for each component.
(d) Apply SSA filtering introduced in the last subsection for each Hankel matrix.

3. Reconstruct the frequency slice use the SSA filtered IMFs.
4. Transform seismic data from f-x domain to t-x domain.

EXAMPLES

In this section, we will use two examples to demonstrate the performance of the proposed method in separating useful reflection signals and ambient random noise. To quantitatively compare the de-noising performance, we use the signal-to-noise ratio (SNR) metric defined below:

$$SNR = 10\log_{10}\frac{\|\mathbf{d}_0\|_2^2}{\|\mathbf{d}_0-\mathbf{d}\|_2^2}\quad , \tag{8}$$

where $\mathbf{d}_0$ is the clean data, and $\mathbf{d}$ is the noisy or de-noised data. Both $\mathbf{d}_0$ and $\mathbf{d}$ are vectorized data (1D vector).

The first synthetic example is a synthetic example, as shown from Figs. 1 to 5. Fig. 1(a) shows the clean data. The noisy data is shown in Fig. 1(b). The SNR of the noisy data is 3.14 dB. Figs. 1(c) and 1(d) shows two zoomed sections from the clean and noisy data. The zooming areas are indicated by the black frameboxes. Fig. 2 shows the comparison between different de-noised data. To compare the performance with the state-of-the-art de-noising algorithms, we use the f-x deconvolution method (Canales, 1984) and the sparsity-based transform-domain thresholding method, i.e., the K-SVD based sparse dictionary learning method (Rubinstein et al., 2008). Figs. 2(a)-(b) correspond to the de-noised data and Figs. 2(c)-(d) correspond to the zoomed data. It is very clear that the result from the proposed method is much cleaner and closer to the exact solution shown in Fig. 1(a). The SNRs for the f-x deconvolution method, the traditional sparsity-based transform-domain thresholding method, and the proposed method are 6.75 dB, 8.34 dB, and 14.76 dB, respectively. Fig. 3 shows a comparison between the noise rejection performance. The noise rejection performance is defined as the difference between noisy data and the de-noised data using different methods (Fig. 4). Note that the proposed method removes obviously more noise than the traditional sparsity-based transform-domain thresholding method. Here, it is worth mentioning that for the sake for losing useful reflection energy, we use a relatively conservative number of IMFs and rank. Because of the unsatisfactory sparsifing performance, we need to use a relatively high threshold value for the traditional sparsity-based transform-domain thresholding method, which results a much weaker removal of noise. Fig. 5a shows a comparison of trace-by-trace amplitude for different data. The proposed method appears to be the closest to the clean data. In a better comparison way, we plot the trace-by-trace error for the three methods in Fig. 5b, where we can see that the f-x deconvolution method causes the largest error and the proposed method causes the smallest error.

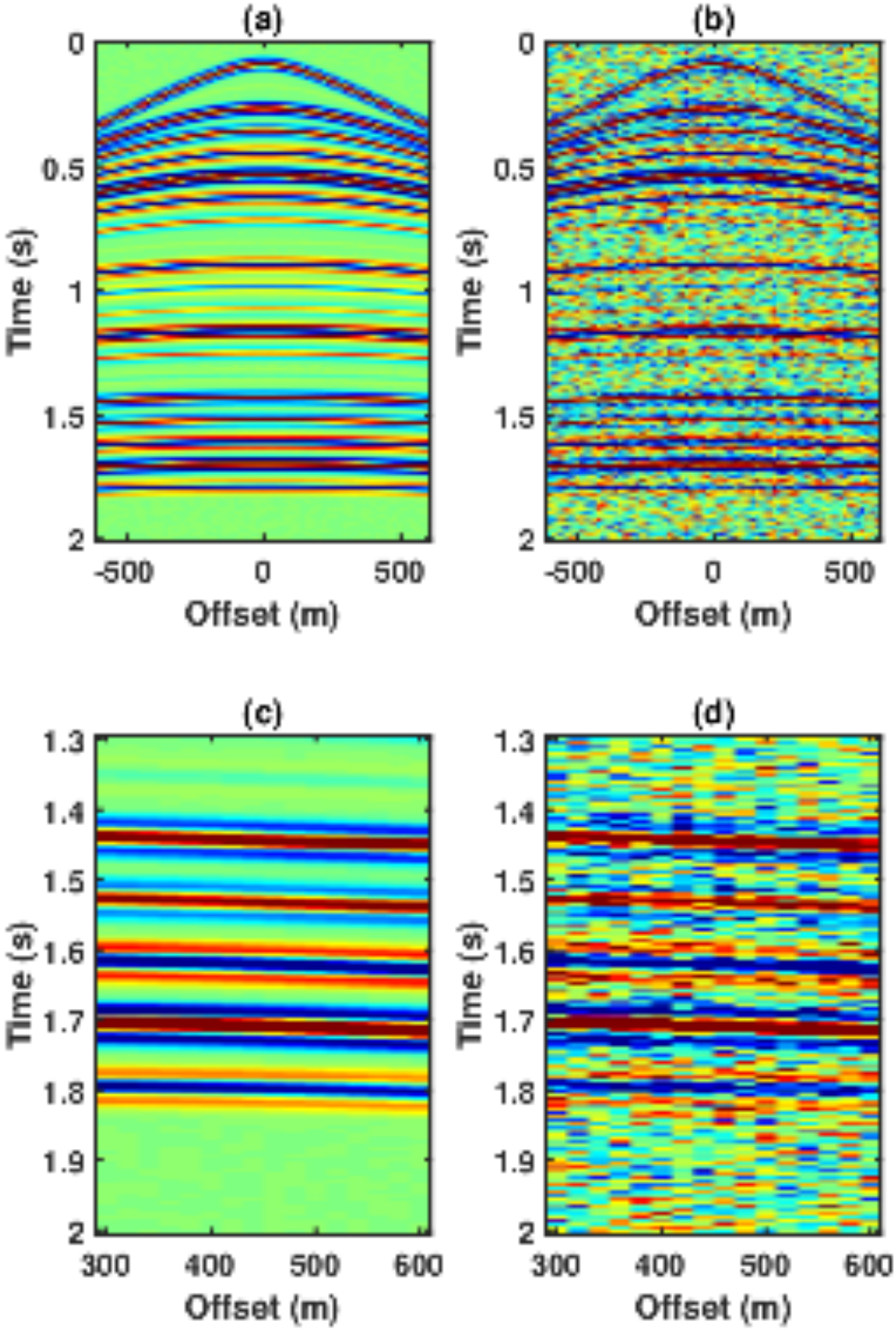

Fig. 1. Synthetic example. (a) Clean data. (b) Noisy data. (c) and (d) Zoomed areas from the frame boxes.

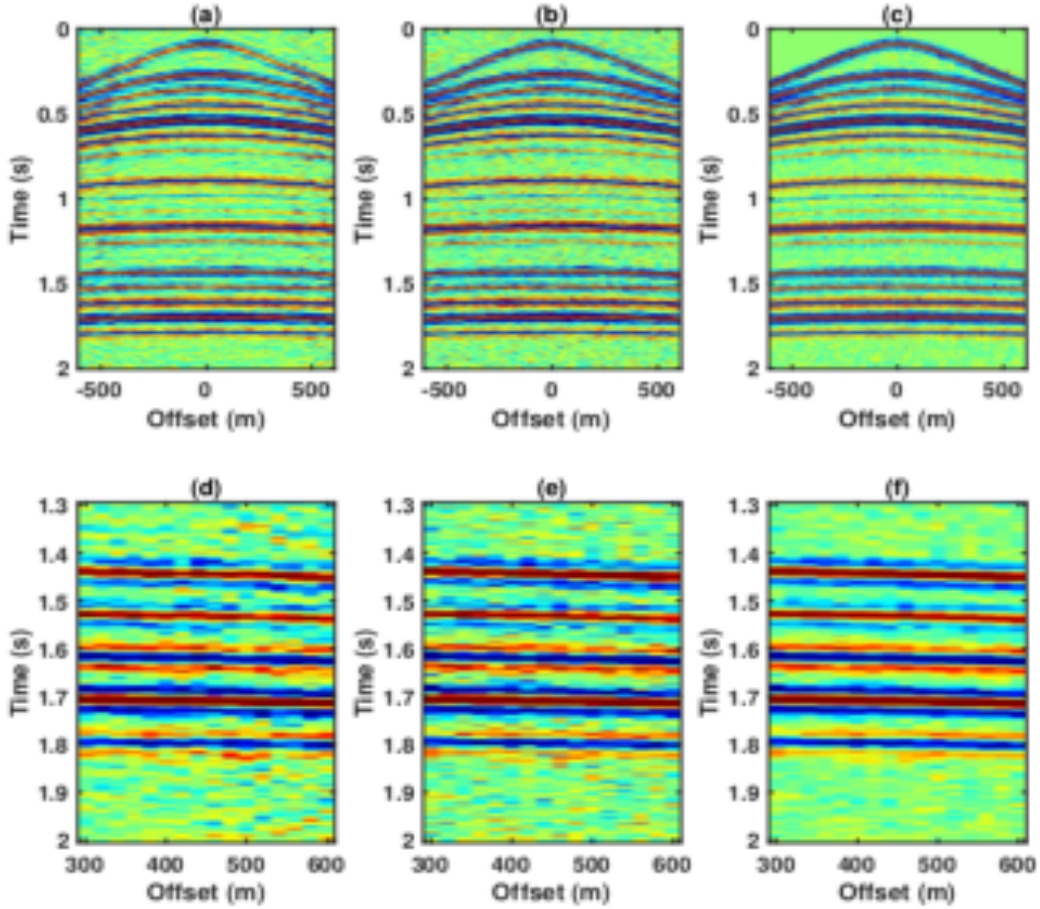

Fig. 2. Synthetic example. (a) Denoised data using the f-x deconvolution method. (b) Denoised data using the traditional sparsity-based transform-domain thresholding method. (c) Denoised data using the proposed method. (d)-(f) Zoomed areas from the frame boxes.

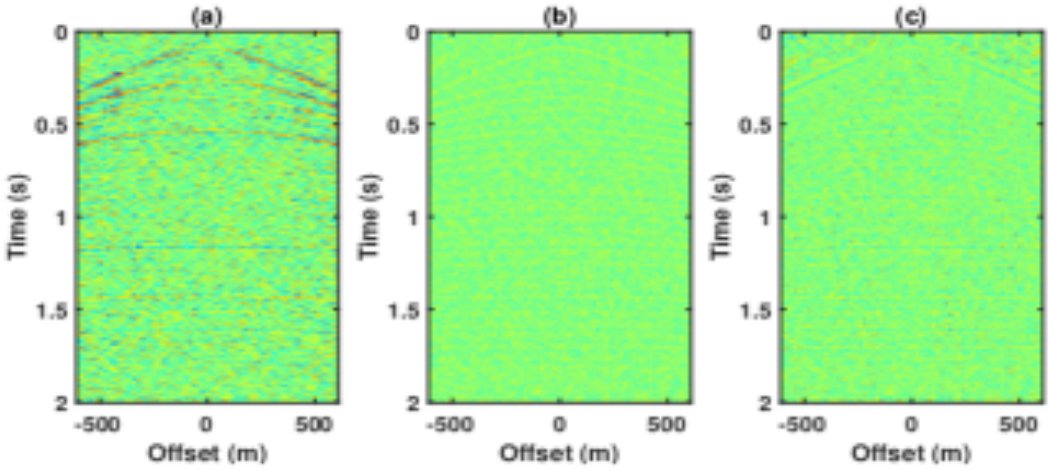

Fig. 3. Synthetic example. (a) Removed noise using the f-x deconvolution method. (b) Removed noise using the traditional sparsity-based transform-domain thresholding method. (c) Removed noise using the proposed method.

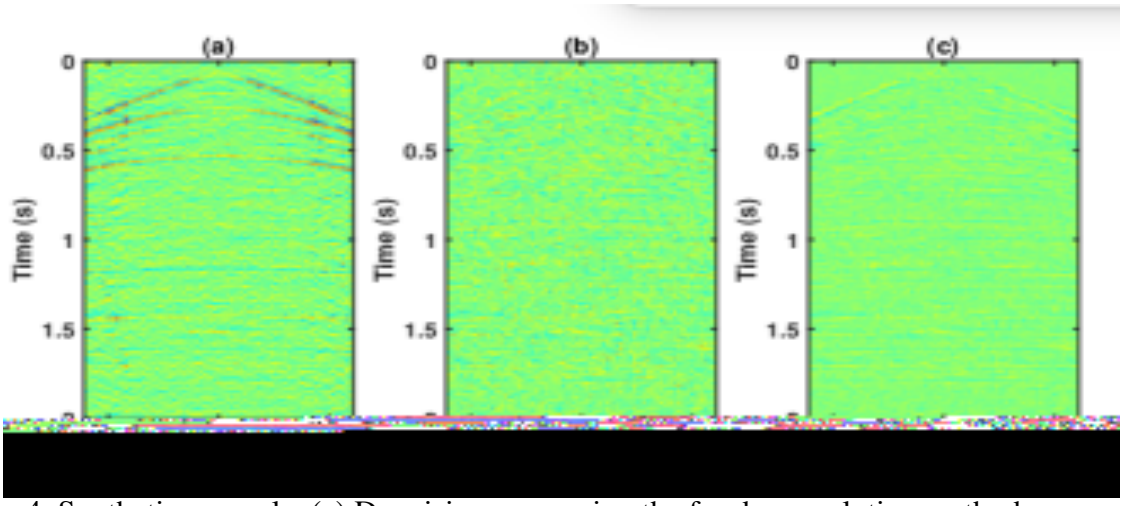

Fig. 4. Synthetic example. (a) Denoising error using the f-x deconvolution method. (b) Denoising error using the traditional sparsity-based transform-domain thresholding method. (c) Denoising error using the proposed method.

Fig. 5. Amplitude and error comparison. (a) Trace-by-trace amplitude comparison. (b) Error comparison. Note that the proposed method obtains the least error.

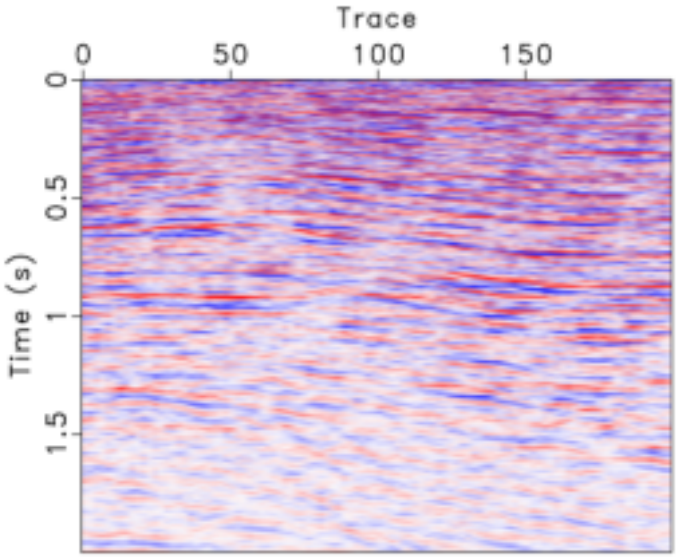

Fig. 6. Field data example.

The next field data example is shown in Fig. 6, which is a post-stack data. Fig. 7 shows the denoised results using four different methods. In this example, we also compare the performance of the proposed method with the that of the traditional SSA filter. Fig. 8 shows the corresponding noise sections. For this example, it seems that all four methods obtain much improved results and the performance of different methods is quite similar. In order to compare the performance in detail and more fairly, we plot the F-K spectra of different denoised results. The F-K spectrum of the raw data is shown in Fig. 9. The F-K spectra corresponding to different methods are shown in Fig. 10. Comparing the F-K spectra of different methods and F-K spectrum of the raw data, it is easy to find that both f-x deconvolution method and the proposed method preserve the useful signals well, but the f-x deconvolution method has some residual spectrum energy around the edges (large wavenumber components). It is obvious that the SSA method and sparsity-based thresholding methods cause significant damages to useful signals. We also plot a comparison of the average spectrum of all the traces for different data (Fig. 11). The red line corresponds to f-x deconvolution method. The pink line corresponds to the SSA method. The blue line corresponds to the sparsity-based thresholding method. The yellow line corresponds to the proposed method. It is quite obvious that the energy preservation of the proposed method in the signal frequency band (20−60 Hz) is quite successful. The proposed method mitigates more high-frequency noise than f-x deconvolution method, which confirms the observation from Fig. 10. In this example, the proposed method preserves more useful energy than the other three methods in the spectrum. This field data further confirms the superior performance of the presented algorithm.

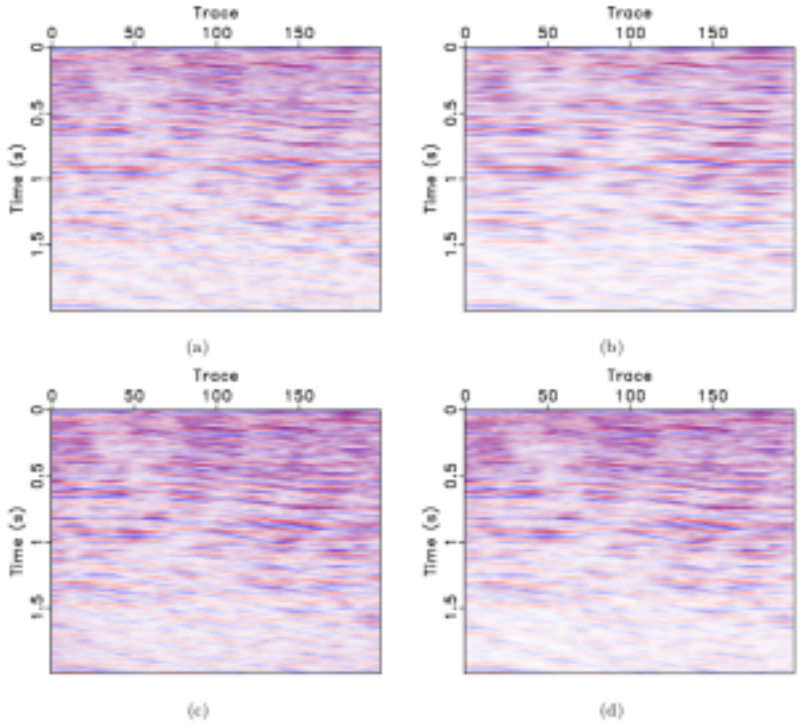

Fig. 7. Denoised data of the field data example using (a) f-x deconvolution method, (b) SSA filter, (c) sparsity-based thresholding method, and (d) the proposed method.

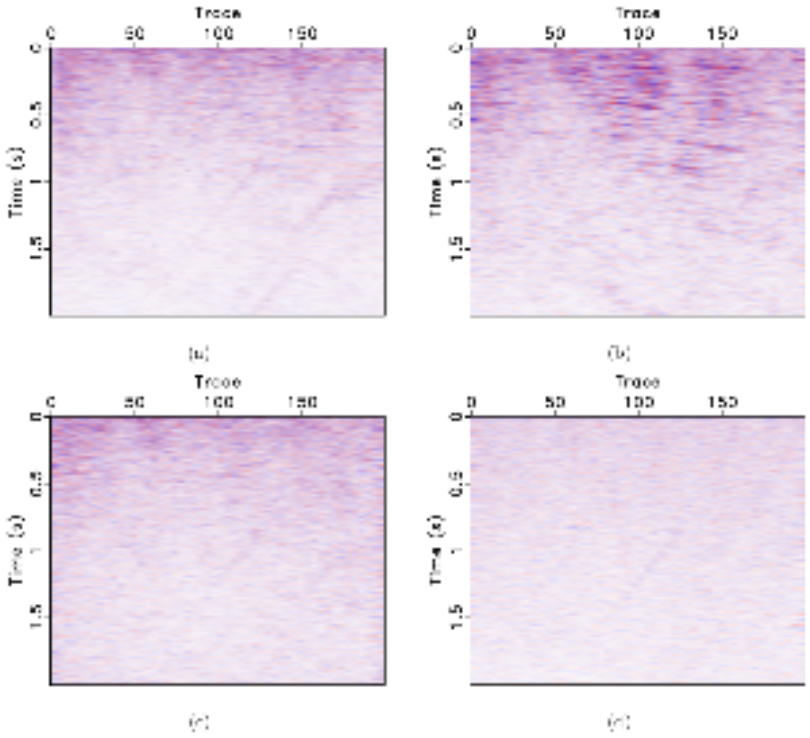

Fig. 8. Removed noise of the field data example using (a) f-x deconvolution method, (b) SSA filter, (c) sparsity-based thresholding method, and (d) the proposed method.

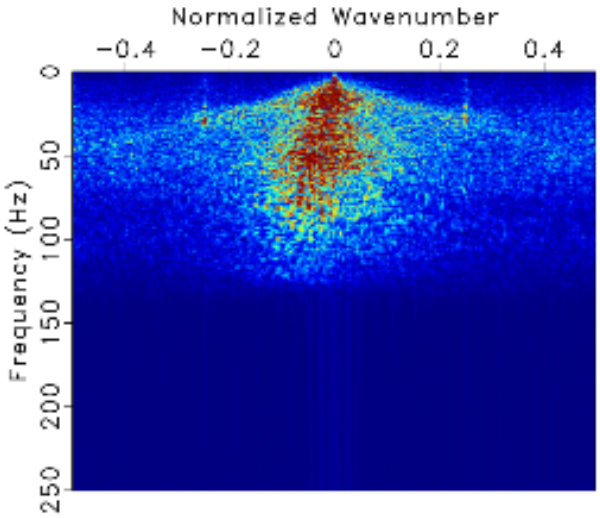

Fig. 9. F-K spectrum comparison of the field data.

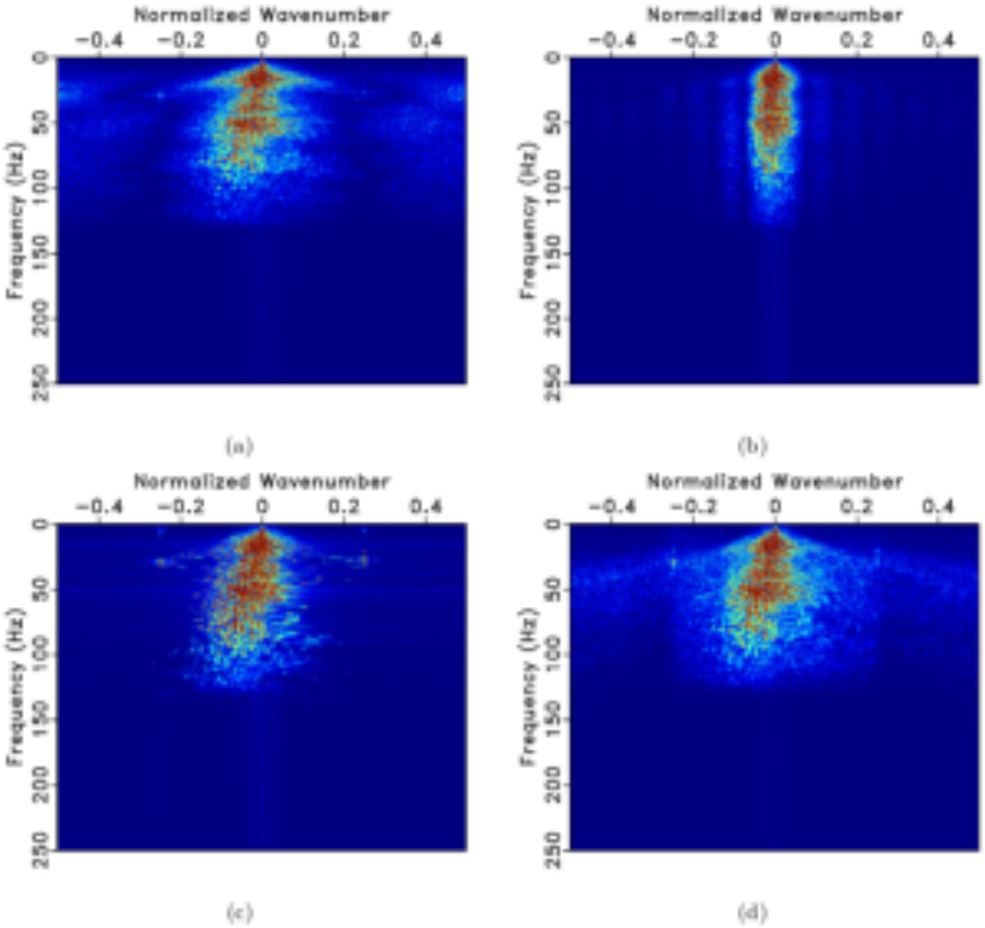

Fig. 10. F-K spectrum comparison of the denoised data in the field data example using (a) f-x deconvolution method, (b) SSA filter, (c) sparsity-based thresholding method, and (d) the proposed method.

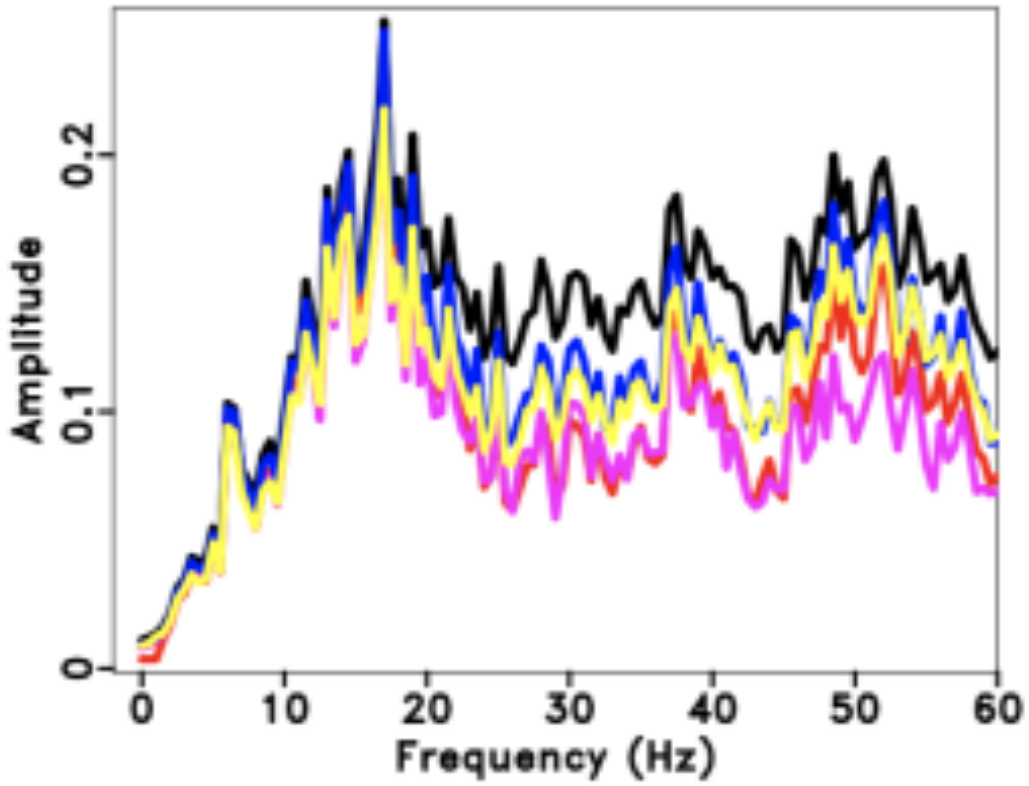

Fig. 11. Comparisons of the average spectrum of all the traces. The black line denotes the average spectrum of raw data. The red line corresponds to f-x deconvolution method method. The pink line corresponds to the SSA method. The blue line corresponds to the sparsity-based thresholding method. The yellow line corresponds to the proposed method. It is clear that the proposed method better preserves the signal energy in the seismic frequency band.

CONCLUSIONS

Under the influence of intensive noise and strong interference, the low-frequency weak seismic signal is difficult to extract completely. The traditional low-rank approximation method assumes the seismic event to be linear and is of low rank. However, for complicated seismic data, this assumption is seldom met. We have proposed a dip-separated filtering strategy to improve the low-rank approximation. The variational mode decomposition (VMD) can be used to decompose the seismic data into different dipping components, each can be better characterized by a low-rank approximation method. We have used both synthetic and field data examples to demonstrate the superior performance of the proposed method compared with the frequency-domain prediction based method and the traditional sparse-transform based method.

ACKNOWLEDGEMENTS

This work was supported by the National Natural Science Foundation of China (No. 61401307), Hebei Province Foundation of Returned oversea scholars (CL201707), Hebei Province Project of Science and Technology R & D (11213565), and Hebei Province Natural Science Foundation (No. E2016202341). The authors are grateful to Weixue Han, Hui Lv and an anonymous reviewer for constructive suggestions which greatly improved the manuscript.

REFERENCES

Bai, M. and Wu, J., 2017. Efficient deblending using median filtering without correct normal moveout - with comparison on migrated images. J. Seismic Explor., 26: 455-479.

Bai, M. and Wu, J., 2018. Seismic deconvolution using iteartive transform-domain sparse inversion. J. Seismic Explor., 27: 103-116.

Bai, M., Wu, J., Xie, J. and Zhang, D., 2018a. Least-squares reverse time migration of blended data with low-rank constraint along structural direction. J. Seismic Explor., 27: 29-48.

Bai, M., Wu, J. and Zhang, H., 2019. Iterative deblending of simultaneous-source data using smoothed singular spectrum analysis. J. Appl. Geophys., 161: 261-269.

Bai, M., Wu, J., Zu, S. and Chen, W., 2018b. A structural rank reduction operator for removing artifacts in least-squares reverse time migration. Comput. Geosci., 117: 9-20.

Bekara, M. and van der Baan, M., 2007. Local singular value decomposition for signal enhancement of seismic data. Geophysics, 72(2): V59-V65.

Canales, L., 1984. Random noise reduction. Expanded Abstr., 54th Ann. Internat. SEG Mtg., Atlanta: 525-527.

Candés, E.J., Demanet, L., Donoho, D.L. and Ying, L., 2006. Fast discrete curvelet transforms. SIAM, Multiscale Model. Simulat., 5: 861-899.

Chen, W., Chen, Y. and Cheng, Z., 2017a. Seismic time-frequency analysis using an improved empirical mode decomposition algorithm. J. Seismic Explor., 26: 367-380.

Chen, W., Chen, Y. and Liu, W., 2016a. Ground roll attenuation using improved complete ensemble empirical mode decomposition. J. Seismic Explor., 25: 485-495.

Chen, W. and Song, H., 2018. Automatic noise attenuation based on clustering and empirical wavelet transform. J. Appl. Geophys., 159: 649-665.

Chen, W., Xie, J., Zu, S., Gan, S. and Chen, Y., 2017b. Multiple reflections noise attenuation using adaptive randomized-order empirical mode decomposition. IEEE Geosci. Remote Sens. Lett., 14: 18-22.

Chen, W., Yuan, J., Chen, Y. and Gan, S., 2017c. Preparing the initial model for iterative deblending by median filtering. J. Seismic Explor., 26: 25-47.

Chen, W., Zhang, D. and Chen, Y., 2017d. Random noise reduction using a hybrid method based on ensemble empirical mode decomposition. J. Seismic Explor., 26: 227-249.

Chen, Y., 2017. Fast dictionary learning for noise attenuation of multidimensional seismic data. Geophys. J. Internat., 209: 21–31.

Chen, Y., 2018a,. Automatic velocity analysis using high-resolution hyperbolic Radon transform. Geophysics, 83(4): A53-A57.

Chen, Y., 2018b. Fast waveform detection for microseismic imaging using unsupervised machine learning. Geophys. J. Internat.,, 215: 1185-1199.

Chen, Y. and Fomel, S., 2015. Random noise attenuation using local signal-and-noise orthogonalization. Geophysics, 80(6): WD1-WD9.

Chen, Y. and Fomel, S., 2018. EMD-seislet transform. Geophysics, 83(1): A27-A32.

Chen, Y., Fomel, S. and Hu, J., 2014. Iterative deblending of simultaneous-source seismic data using seislet-domain shaping regularization. Geophysics, 79(5): V179-V189.

Chen, Y., Huang, W., Zhou, Y., Liu, W. and Zhang, D., 2018. Plane-wave orthogonal polynomial transform for amplitude-preserving noise attenuation. Geophys. J. Internat., 214: 2207-2223.

Chen, Y. and Ma, J., 2014. Random noise attenuation by f-x empirical mode decomposition predictive filtering. Geophysics, 79(3): V81-V91.

Chen, Y., Ma, J. and Fomel, S., 2016b. Double-sparsity dictionary for seismic noise attenuation. Geophysics, 81(2): V17-V30.

Chen, Y., Zhang, D., Jin, Z., Chen, X., Zu, S., Huang, W. and Gan, S., 2016c. Simultaneous denoising and reconstruction of 5D seismic data via damped rank-reduction method. Geophys. J. Internat.,, 206: 1695-1717.

Chen, Y., Zu, S., Wang, Y. and Chen, X., 2019. Deblending of simultaneous-source data using a structure-oriented space-varying median filter. Geophys. J. Internat., 216: 1214-1232.

Dragomiretskiy, K. and Zosso, D., 2014. Variational mode decomposition. IEEE Transact. Sign. Process., 62: 531-544.

Fomel, S. and Liu, Y., 2010. Seislet transform and seislet frame. Geophysics, 75(3): V25-V38.

Gan, S., Wang, S., Chen, Y. and Chen, X., 2016a. Simultaneous-source separation using iterative seislet-frame thresholding. IEEE Geosci. Remote Sens. Lett., 13: 197-201.

Gan, S., Wang, S., Chen, Y., Chen, X., Huang, W. and Chen, H., 2016b. Compressive sensing for seismic data reconstruction via fast projection onto convex sets based on seislet transform. J. Appl. Geophys., 130: 194-208.

Gan, S., Wang, S., Chen, Y., Chen, X. and Xiang, K., 2016c. Separation of simultaneous sources using a structural-oriented median filter in the flattened dimension. Comput. Geosci., 86: 46-54.

Gan, S., Wang, S., Chen, Y., Qu, S. and Zu, S., 2016d. Velocity analysis of simultaneous-source data using high-resolution semblance-coping with the strong noise. Geophys. J. Internat., 204: 768-779.

Gan, S., Wang, S., Chen, Y., Zhang, Y. and Jin, Z., 2015. Dealiased seismic data interpolation using seislet transform with low-frequency constraint. IEEE Geosci. Remote Sens. Lett., 12: 2150-2154.

Huang, N.E., Shen, Z., Long, S.R., Wu, M.C., Shih, H.H., Zheng, Q., Yen, N.-C., Tung, C.C. and Liu, H.H., 1998. The empirical mode decomposition and the Hilbert spectrum for nonlinear and non-stationary time series analysis. Proc. Roy. Soc. London, Series A, 454: 903-995.

Huang, W., Wang, R., Chen, X. and Chen, Y., 2017a. Double least squares projections method for signal estimation. IEEE Transact. Geosci. Remote Sens., 55: 4111-4129.

Huang, W., Wang, R., Yuan, Y., Gan, S. and Chen, Y., 2017b. Signal extraction using randomized-order multichannel singular spectrum analysis. Geophysics, 82(2): V59-V74.

Huang, W., Wang, R., Zhang, D., Zhou, Y., Yang, W. and Chen, Y., 2017c. Mathematical morphological filtering for linear noise attenuation of seismic data. Geophysics, 82(6): V369-V384.

Huang, W., Wang, R., Zu, S. and Chen, Y., 2017d. Low-frequency noise attenuation in seismic and microseismic data using mathematical morphological filtering. Geophys. J. Internat., 211: 1318-1340.

Huang, W., Wang, R. and Chen, Y., 2018. Regularized non-stationary morphological reconstruction algorithm for weak signal detection in micro-seismic monitoring. Methodology. Geophys. J. Internat., 213: 1189-1211.

Li, H., R. Wang, S. Cao, Y. Chen, and W. Huang, 2016a. A method for low-frequency noise suppression based on mathematical morphology in microseismic monitoring. Geophysics, 81(3): V159-V167.

Li, H., Wang, R., Cao, S., Chen, Y., Tian, N. and Chen, X., 2016b. Weak signal detection using multiscale morphology in microseismic monitoring. J. Appl. Geophys., 133: 39-49.

Liu, G., Chen, X., Du, J. and Wu, K., 2012. Random noise attenuation using f-x regularized nonstationary autoregression. Geophysics, 77(2): V61-V69.

Liu, W., Cao, S. and Chen, Y., 2016a. Applications of variational mode decomposition in seismic time-frequency analysis. Geophysics, 81(5): V365-V378.

Liu, W., Cao, S. and Chen, Y., 2016b. Seismic time-frequency analysis via empirical wavelet transform. IEEE Geosci. Remote Sens. Lett., 13: 28-32.

Liu, W., Cao, S., Gan, S., Chen, Y., Zu, S. and Jin, Z., 2016c. One-step slope estimation for dealiased seismic data reconstruction via iterative seislet thresholding. IEEE Geosci. Remote Sens. Lett., 13: 1462-1466.

Liu, W., Cao, S., Jin, Z., Wang, Z. and Chen, Y., 2018. A novel hydrocarbon detection approach via high-resolution frequency-dependent AVO inversion based on variational mode decomposition. IEEE Transact. Geosci. Remote Sens., 56: 2007-2024.

Liu, W., Cao, S., Wang, Z., Kong, X. and Chen, Y., 2017. Spectral decomposition for hydrocarbon detection based on YMD and Teager-Kaiser energy. IEEE Geosci. Remote Sens. Lett., 14: 539-543.

Lv, H. and Bai, M., 2018. Learning dictionary in the approximately flattened structure domain. J. Appl. Geophys., 159: 522-531.

Rubinstein, R., Zibulevsky, M. and Elad, M., 2008. Efficient implementation of the K-SVD algorithm using batch orthogonal matching pursuit. Techn. Rep.

Siahsar, M.A.N., Abolghasemi, V. and Chen, Y., 2017a. Simultaneous denoising and interpolation of 2D seismic data using data-driven non-negative dictionary learning. Sign. Process., 141: 309-321.

Siahsar, M.A.N., Gholtashi, S., Kahoo, A.R., Chen, W. and Chen, Y., 2017b. Data-driven multi-task sparse dictionary learning for noise attenuation of 3D seismic data. Geophysics, 82(6): V385-V396.

Siahsar, M.A.N., Gholtashi, S., Olyaei, E., Chen, W. and Chen, Y., 2017c. Simultaneous denoising and interpolation of 3D seismic data via damped data-driven optimal singular value shrinkage. IEEE Geosci. Remote Sens. Lett., 14: 1086-1090.

Vautard, R., Yiou, P. and Ghil, M., 1992. Singular-spectrum analysis: A toolkit for short, noisy chaotic signals. Physica D: Nonlin. Phenom., 58: 95-126.

Wang, Y., Ma, X., Zhou, H. and Chen, Y., 2018. L1-2 minimization for exact and stable seismic attenuation compensation. Geophys. J. Internat., 213: 1629-1646.

Wang, Y., Zhou, H., Zu, S., Mao, W. and Chen, Y., 2017. Three-operator proximal splitting scheme for 3D seismic data reconstruction. IEEE Geosci. Remote Sens. Lett., 14: 1830-1834.

Wu, J. and Bai, M., 2018a. Attenuating seismic noise via incoherent dictionary learning. J. Geophys. Engineer., 15: 1327.

Wu, J. and Bai, M., 2018b. Fast principal component analysis for stacking seismic data. J. Geophys. Engineer., 15: 295-306.

Wu, J. and Bai, M., 2018c. Incoherent dictionary learning for reducing crosstalk noise in least-squares reverse time migration. Comput. Geosci., 114: 11-21.

Wu, J. and Bai, M., 2018d. Stacking seismic data based on principal component analysis. J. Seismic Explor., 27: 331-348.

Xue, Y., Chang, F., Zhang, D. and Chen, Y., 2016. Simultaneous sources separation via an iterative rank-increasing method. IEEE Geosci. Remote Sens. Lett., 13: 1915-1919.

Zhang, D., Chen, Y., Huang, W. and Gan, S., 2016. Multi-step damped multichannel singular spectrum analysis for simultaneous reconstruction and denoising of 3D seismic data. J. Geophys. Engineer., 13: 704-720.

Zhang, D., Zhou, Y., Chen, H., Chen, W., Zu, S. and Chen, Y., 2017. Hybrid rank-sparsity constraint model for simultaneous reconstruction and denoising of 3D seismic data. Geophysics, 82(5): V351-V367.

Zu, S., Zhou, H., Chen, Y., Qu, S., Zou, X., Chen, H. and Liu, R., 2016. A periodically varying code for improving deblending of simultaneous sources in marine acquisition. Geophysics, 81(3): V213-V225.

Zu, S., Zhou, H., Chen, H., Zheng, H. and Chen, Y., 2017a. Two field trials for deblending of simultaneous source surveys: why we failed and why we succeeded? J. Appl. Geophys., 143: 182–194.

Zu, S., Zhou, H., Li, Q., Chen, H., Zhang, Q., Mao, W. and Chen, Y., 2017b. Shot-domain deblending using least-squares inversion. Geophysics, 82(4): V241-V256.

Zu, S., Zhou, H., Mao, W., Zhang, D., Li, C., Pan, X. and Chen, Y., 2017c. Iterative deblending of simultaneous-source data using a coherency-pass shaping operator. Geophys. J. Internat., 211: 541-557.